Synthesis, Structure, and Physical Properties of a New Phenalenyl-Based Neutral Radical Crystal: Correlation between Structure and Transport Properties in Carbon-Based Molecular Conductors

X. CHI,[1] M. E. ITKIS,[1] F. S. THAM,[1] R. T. OAKLEY,[2] A. W. CORDES,[3] R. C. HADDON[1]

[1]*Departments of Chemistry and Chemical & Environmental Engineering, University of California, Riverside, CA 92521-0403*

[2]*Department of Chemistry, University of Waterloo, Waterloo, Ontario N2L 3G1, Canada*

[3]*Department of Chemistry and Biochemistry, University of Arkansas, Fayetteville, AR 72701*

Received 11 June 2003; accepted 13 June 2003

DOI 10.1002/qua.10759

ABSTRACT: A new class of phenalenyl-based neutral radical molecular conductors has recently been reported; a distinctive feature of these molecular solids is the absence of the well-defined conducting pathway(s) that are characteristic of the organic charge-transfer salts. These radicals do not stack in the solid state, and the requisite carbon–carbon contacts are all larger than the sum of the van der Waals distances. Magnetic susceptibility measurements show that these compounds usually exist as isolated free radicals with one spin per molecule (at least over some temperature range), apparently supporting the idea that there is little interaction between the molecules in the solid state. Nevertheless, these radicals show the highest conductivity (σ_{RT} = 0.05 S/cm) of any neutral organic solid and the conduction mechanism is at present unresolved. In this article we report a structurally related radical with a resistivity five orders of magnitude higher than that of the previously reported radicals. We analyze the crystallographic and electronic structure of this solid in detail and point out some of the challenges that remain in relating structure, magnetism, and conductivity in this new class of organic solids. Int J Quantum Chem 95: 853–865, 2003

Key words: phenalenyl; neutral radical; molecular conductor; crystal packing

Correspondence to: R. C. Haddon; e-mail: robert.haddon@ucr.edu

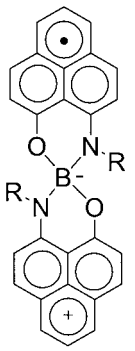

1. R=Et
2. R=Pr
3. R=Bu
4. R=Pt
5. R=Hx

SCHEME 1.

Introduction

In the last 30 years a large number of organic conductors and superconductors have been synthesized based on TTF (Tetrathiafulvalene) derivatives and C_{60} [1]. These highly conducting compounds are charge-transfer salts, where the charge carriers are generated by forming radical ions. Recently, a single-component organometallic molecular metal was reported [2].

Some time ago, organic neutral radicals were suggested to be candidates to form an intrinsic molecular conductor, in which the unpaired electrons of the neutral radicals may serve as charge carriers [3]. Sulfer-nitrogen radicals were the first class of neutral radicals to show conductivity based on this principle [4]. Recently, we reported a series of spiro-biphenalenyl boron neutral radicals (Scheme 1) [5–7]. Although these compounds differ only in the length of the alkyl groups (R), they show significantly different physical properties. For example, hexyl radical **5** exists as monomers in the solid state with the highest conductivity at room temperature (σ_{RT} = 0.05 S/cm) of any neutral organic compound reported [5]. Both radicals **1** and **3** form face–face π-dimers in which the phenalenyl (PLY) ring systems overlap so that there is registry of the spin-bearing carbon atoms [6]. These crystals undergo phase transitions from high-temperature paramagnetic states to low-temperature diamagnetic states, accompanied by an increase in conductivities of two orders of magnitude. Their room temperature conductivities (σ_{RT} = 0.01 and 0.024 S/cm, respectively) are comparable with that of hexyl radical. Radical **2** also forms face–face σ-dimers. Nevertheless, its conductivity (σ_{RT} = 1.4×10^{-6} S/cm) is four orders of magnitude lower than those of the other three radicals in the series [7]. By careful examination of the molecular packing of the radicals [7], we found that within the crystal lattice of the better conductors, such as radical **5,** there exist effective conducting pathways formed by the interaction between the PLY units of the neighboring molecules. These PLY units lie directly above each other, and the angles between them are significantly less than 90° (the strongest interaction occurs when the two PLYs are parallel and and the active carbon atoms are superimposed) [7]. Moreover, these interactions form a continuous pathway throughout the lattice. On the other hand, radical **2** does not form an effective conducting pathway in the lattice because the PLY units of neighboring π-dimers lie either side by side (weak interaction) or perpendicular to each other (also a weak interaction). The π–π interaction within a dimer is strong, but this interaction cannot continue throughout the lattice.

The fact that the transport property of a solid is determined by the molecular packing in the lattice, and that the packing structures of these radicals are significantly affected by simply changing the length of the alkyl group, prompted us to explore more compounds in the series. Here, we report the synthesis, structure, and physical properties of radical **4.** We show that in this crystal the molecules also have π–π interactions (leading to a paramagnetic π-dimer) but in a different manner than those found in **1, 2,** and **3.** Moreover, the PLY units of the neighboring dimer pairs are either perpendicular to or to the side of each other. This kind of molecular orientation and arrangement has been found to lead to ineffective conducting pathways [7], and this compound is found to have a low conductivity similar to that of radical **2.**

Materials and Methods

MATERIALS

Boron trichloride (Aldrich), sodium tetraphenylborate (Aldrich), and cobaltocene (Strem) were all commercial products and were used as received. 9-Hydroxyphenalenone was synthesized according to the literature procedures [8, 9]. Toluene was distilled from sodium benzophenone ketyl immediately before use. Acetonitrile was distilled from P_2O_5 and then redistilled from K_2CO_3 immediately before use.

N-PENTYL-9-AMINO-1-PHENALENONE

A mixture of 9-hydroxyphenalenone (0.98 g, 0.005 mol) and pentylamine (10 mL) was refluxed

for 20 h in Ar. The solvent was removed by rotary evaporator and the yellow solid was purified by column chromatography on Al_2O_3 with $CHCl_3$ (1.1 g, 83%); leaflets were from heptane, m.p. 77–78°C. ^{1}H-NMR (CD_3CN): δ 12.22 (b, 1H), 8.05 (d, 1H), 7.85–7.95 (m, 3H), 7.43 (t, 1H), 7.34 (d, 1H), 6.85 (d, 1H), 3.57 (d of t, 2H), 1.68–1.80 (m, 2H), 1.32–1.61 (m, 4H), 0.8 (t, 3H). Calcd for $C_{18}H_{19}ON$: C, 81.48; H, 7.22; N, 5.28. Found: C, 80.98; H, 7.33; N, 5.28.

PREPARATION OF 4^+, CL^-

N-Pentyl-9-amino-1-phenalenone (0.8 g, 0.003 mol) in toluene (100 mL) was treated with boron trichloride in dichloromethane (1.3 mL, 0.001 mol) under argon in the dark, and the mixture was refluxed overnight. The yellow solid was isolated by filtration (0.68 g, 90%). When a melting point determination was attempted, the salt turned black (~150°C).

PREPARATION OF 4^+, BPh_4^-

A solution of 0.5 g Na^+, BPh_4^- (1.60 mmol) in 10 mL MeOH was added to a solution of $\mathbf{4}^+$, Cl^-, (0.58 g, 1.05 mmol) in 40 mL MeOH. The mixture was stirred for 5 min, and an orange, crystalline solid formed that was isolated by filtration. The orange product was purified by recrystallization from a dichloromethane–methanol mixture. Yield: 0.75 g (88%). When a melting point determination was attempted, the salt turned black (~150°C). ^{1}H-NMR (acetone): δ 8.74 (d, 2H), 8.62 (d, 2H), 8.52 (d, 2H), 8.45 (d, 2H), 7.93 (t, 2H), 7.72 (d, 2H), 7.60 (d, 2H), 7.27–7.41 (m, 8H), 6.92 (t, 8H), 6.76 (t, 4H), 3.82–4.03 (b, 2H), 3.45–3.65 (b, 2H), 1.77–2.01 (m, 4H), 1.02–1.34 (m, 8H), 0.71 (t, 6H). Anal. calcd for $C_{60}H_{56}O_2N_2B_2$: C, 84.21; H, 6.54; N, 3.27; B, 2.34. Found: C, 84.47; H, 6.63; N, 3.19; B, 2.38.

CRYSTALLIZATION OF 4

An invertable H cell with a glass D frit was loaded in a dry box. A solution of 86 mg of $\mathbf{4}^+$, BPh_4^- (0.1 mmol) in 20 mL dry CH_3CN was placed in one container and 20 mg of $CoCp_2$ (0.1 mmol) dissolved in 20 mL dry CH_3CN in the other container. The containers were attached to the inverted H cell in the dry box. The H cell was removed from the dry box and attached to a vacuum line and the containers taken through three cycles of freeze, pump, and thaw to degas the solutions. The H cell was inverted, and the solutions were allowed to diffuse through the glass frit. After sitting in the dark for 1 week the cell yielded 40 mg (70%) of black needles. Anal. calcd for $C_{36}H_{36}O_2N_2B$: C, 80.15; H, 6.73; N, 5.19; B, 2.00. Found: C, 79.99; H, 6.55; N, 5.40; B, 2.08.

MAGNETIC SUSCEPTIBILITY MEASUREMENTS

The magnetic susceptibility was measured over the temperature range 4–350 K on a George Associates Faraday balance operating at 0.5 T.

ELECTRICAL CONDUCTIVITY MEASUREMENTS

The single-crystal conductivity was measured in a custom-made helium variable-temperature probe in a four-probe configuration. The in-line contacts were made with silver paint.

OPTICAL MEASUREMENTS

The transmission spectra on a single crystal of **4** were measured using a Continuum Thermo-Nicolet FT-IR microscope integrated with a Nexus-670 FT-IR Nicolet spectrometer.

EHT CALCULATIONS

The band structure calculations made use of a modified version of the EHT band structure program. The parameter set is chosen to provide a reasonably consistent picture of bonding in heterocyclic organic compounds [10, 11].

Results and Discussion

PREPARATION OF RADICAL 4

The synthesis of the precursor ($\mathbf{4}^+$, BPh_4^-) followed the same procedure that was used for the other salts in the series [5–7]. Table I lists the results of the cyclic voltammetric experiments carried out on salts $\mathbf{1}^+$, $\mathbf{2}^+$, $\mathbf{3}^+$, and $\mathbf{5}^+$ (with BPh_4^- as the counterion).

It is immediately apparent that the electrochemistry of these salts is virtually unaffected by the alkyl groups. Although we did not perform cyclic voltammetry measurement on salt ($\mathbf{4}^+$, BPh_4^-), it is certain that its first reduction potential should be at ~ -0.74 V and the second potential should be at ~ -1.11 V. Therefore, in accordance with the other radicals, we were confident that cobaltocene (oxidation potential, $E^{1/2} = -0.91$ V) [12] could be

TABLE I

Half-wave potentials[a] and the disproportionation potentials of various tetraphenylborate salts.

Cation	$E_1^{1/2}$	$E_2^{1/2}$	ΔE	Ref.
$\mathbf{1}^+$	−0.75	−1.10	0.35	[6]
$\mathbf{2}^+$	−0.747	−1.102	0.36	[7]
$\mathbf{3}^+$	−0.733	−1.110	0.36	[6]
$\mathbf{5}^+$	−0.741	−1.108	0.37	[5]

[a] In acetonitrile, referenced to SCE (Saturated Calomel Electrode) via internal ferrocene.

used to reduce $\mathbf{4}^+$ to the radical **4,** but not further to the anion $\mathbf{4}^-$**.** In the H cell, this radical crystallizes more slowly than other compounds in the series, and it is important to let the cell stand for a longer time (crystals start to form after 3 days).

X-RAY CRYSTAL STRUCTURE OF RADICAL 4

The crystal data for radical **4** are listed in Table II and an ORTEP drawing with the atom numbering is shown in Figure 1. Figure 2 shows a unit cell containing eight molecules or four pairs of enantiomers.

Each pair of enantiomers forms a π-dimer. For example, molecules H and I (Fig. 2) have face-to-face π–π interactions. We reported that radicals **1, 2,** and **3** also form π-dimers [6, 7]. These compounds are paramagnetic when the mean plane separations are larger than ~3.3 Å, and are referred to as paramagnetic π-dimers; at low temperatures, the mean plane separations become shorter (~3.1 Å), and the compounds become diamagnetic and at this point they are referred to as diamagnetic π-dimers. The mean plane separation of **4** at the measured temperature (223 K) is about 3.5 Å, larger than the separations of **1, 2,** and **3** in their paramagnetic states.

It is important to compare the overlaps of the singly occupied molecular orbitals (SOMOs) of the PLY units that have face-to-face π–π interactions. In compounds **1, 2,** and **3,** the active carbon atoms (with most of the spin density in SOMO) are almost completely superimposed, which ensures the optimal overlap of the SOMOs of the two PLY units within the dimers. A typical diagram of this overlap is shown in Figure 3.

However, the π–π overlap in **4** is much different (Fig. 4). Only a subset of the PLY ring carbon atoms lie directly on top of each other, and none of the active carbon atoms is superimposed.

Because the overlap of the SOMOs of **4** is poor and the mean plane separation is large, it is questionable whether the interaction between the two PLYs is significant. We have shown in a previous article that the location of the unpaired electron in each molecule is strongly affected by the π–π interaction between neighboring molecules [13]. For example, in radical **5** the molecules do not have π–π interactions and the unpaired electrons delocalize over through the two halves of the molecules. In radicals **1** and **3,** when the π–π interactions are moderate (paramagnetic π-dimers), the two unpaired electrons of π-dimer pair avoid each other and reside in the two ends of the molecules that have no π–π interactions. When the π–π interactions are strong (diamagnetic π-dimers), the two electrons come together and reside in the central (overlapping) pair of PLYs and spin pair. This interpretation was deduced by a comparison of the bond length change in the radicals (referenced to the cations) with the signs of the partial bond order of the SOMOs. This is because the signs of the partial bond order of the SOMOs determines the bonding or antibonding character of the SOMOs. Therefore, population of the SOMO causes those bonds with bonding character (positive sign of the partial bond order) to be strengthened and the bond length shortened; likewise, those bonds with antibonding character (negative sign of the partial bond order) are weakened and the bond length is lengthened. We performed a similar analysis on radical **4,** and the results are listed in Table III.

TABLE II

Crystal data for 4.

Formula	$BO_2N_2C_{36}H_{36}$
fw (formula weight)	539.48
Space group	C2/c
Crystal system	Monoclinic
a (Å)	27.071 (3)
b (Å)	10.258 (1)
c (Å)	20.794 (2)
β (°)	90.230 (2)
V (Å^3)	5774 (1)
Z	8
Temperature (K)	223 (2)
μ (mm^{-1})	0.076
Theta range for data collection	1.50–28.28
Refine data (all)	7164
Parameters refined	372
Goodness-of-fit on F2	1.012
R indices (all data)	0.086
R for reflections with $I > 2\sigma(I)$	0.046
Mean plane separation (Å)	3.51 (1)

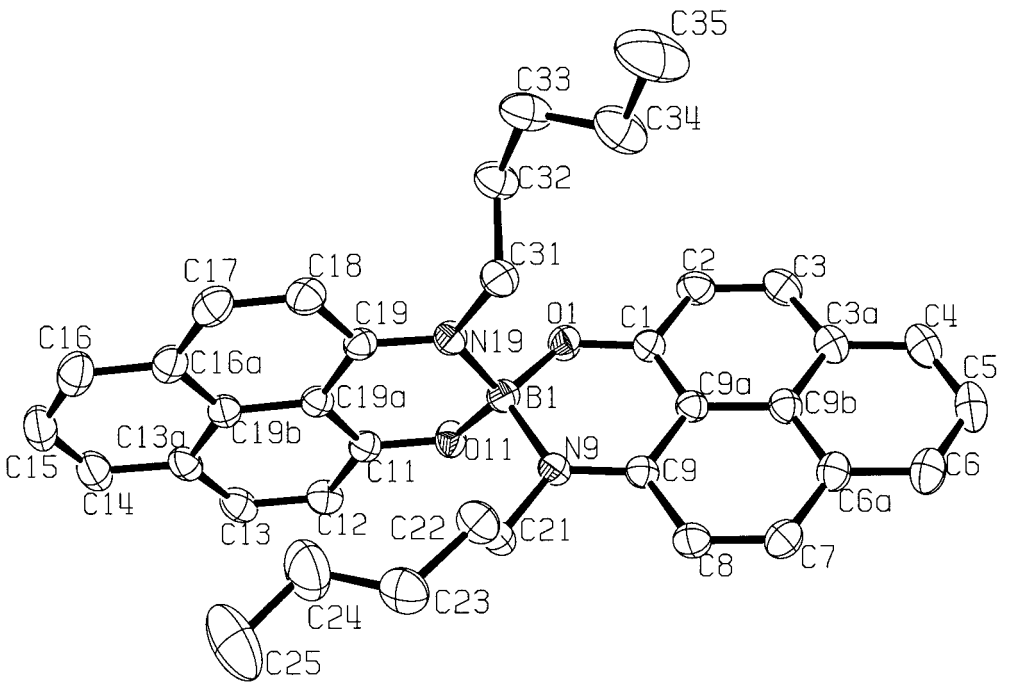

FIGURE 1. ORTEP drawing and the atom numbering of **4.** The hydrogen atoms are omitted.

The bottom row of Table III shows that the standard deviation of the bond length differences between the two halves of the molecule **4** is 0.023, much larger than that of $\mathbf{3}^+$, indicating that the two PLYs of molecule **4** are different. This is confirmed by the standard deviations of the bond length changes of **4** referenced to $\mathbf{3}^+$ (columns 5 and 6). The SD of the bond length changes of the ring containing C1–C9 (top half of column 6) is 0.003, indicating that these bonds are comparable to those of the cation. These bonds do not change, or the SOMO of this PLY unit is almost completely empty. On the other hand, the SD of the bond length changes of the other half of the molecule (bottom half of column 6) is 0.017, indicating that these bonds are significantly different from those of $\mathbf{3}^+$. By comparing columns 5 and 7, it is obvious that the bond length changes of the ring containing C11—C19 (bottom half of column 5) all match perfectly with the sign of partial bond order for SOMO, whereas the changes of the other half do not. Because the PLY unit containing C1—C9 has π–π interaction with the other molecule, we conclude that π–π interaction in radical **4** is significant and the two unpaired electrons in the π-dimer avoid each other and reside mainly in the two distant ends of the molecules where there is no π–π interaction. On the basis of the crystallography, we expect that compound **4** is paramagnetic at the temperature where the structure is determined (223 K).

MOLECULAR INTERACTIONS IN THE LATTICE

To show conductivity, a solid must not only possess charge carriers but also provide effective conducting pathways. We have shown in a previous article [7] that the carbon-based neutral radicals have effective conducting pathways, but in a manner that is much more subtle than those that exist in the charge-transfer salts based on TTF derivatives or spherical C_{60}. Thus, side-by-side arrangement of the PLY units allows no overlap of the SOMOs and the interaction is negligible. The strongest interaction occurs when the two PLY units are not only on top of but also parallel to each other (where a π-dimer is formed). The interaction gets weaker when the angle between them increases, and when they are perpendicular to each other (90°) the interaction is weakest. In crystal of **5,** the strongest interaction between neighboring PLY units involves angles of 75–80°, and these interactions continue throughout the whole solids. In crystals of **2,** however, the PLY units of neighboring π-dimers are either perpendicular to each other or in a side-by-side arrangement. Thus, the interactions of the PLY

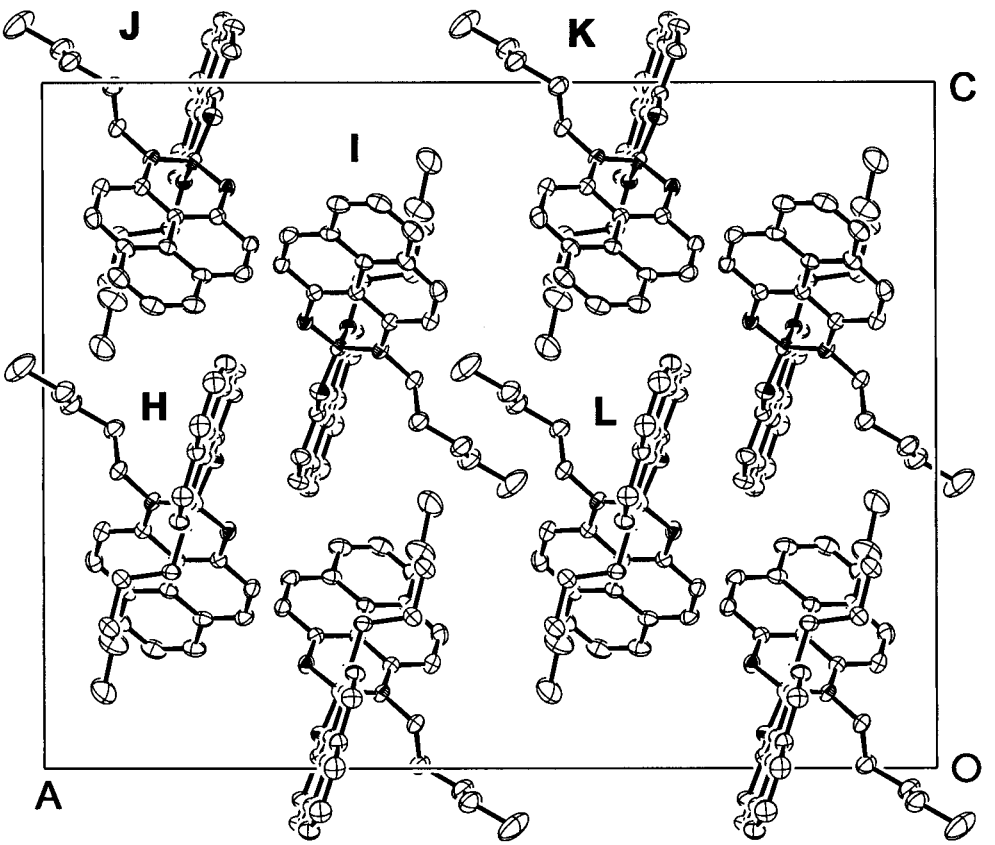

FIGURE 2. Unit cell of **4** containing eight molecules or four pairs of enantiomers.

units in crystals of **2** that continue throughout the lattice are all weak and there is no effective conducting pathway. We can now perform a similar examination on crystal of **4.**

There are eight molecules in the unit cell, as shown in Figure 2. Each molecule forms a column along the b direction (Fig. 5). Because the PLY units of neighboring molecules in the column are perpen-

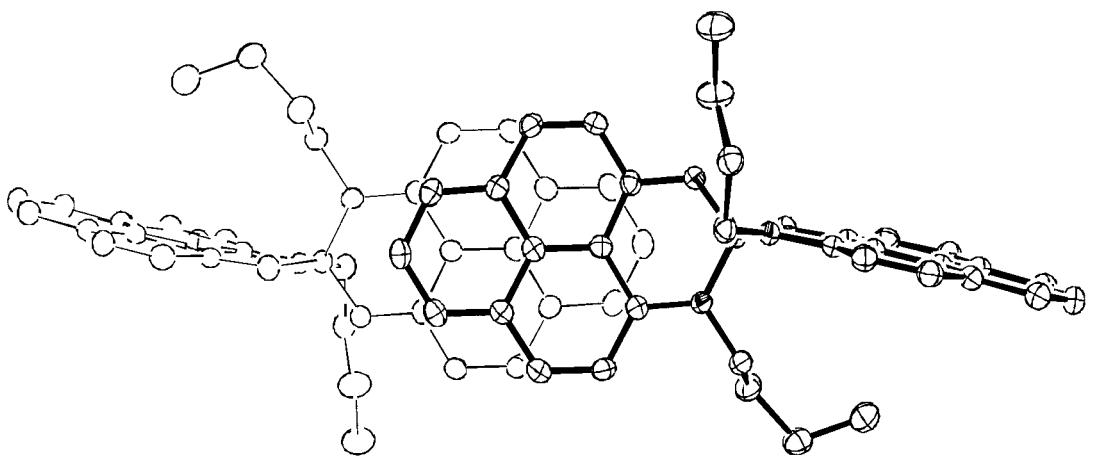

FIGURE 3. Overlap within a π-dimer of compound **3** [13]. The π—π overlap in compounds **1** and **2** are similar.

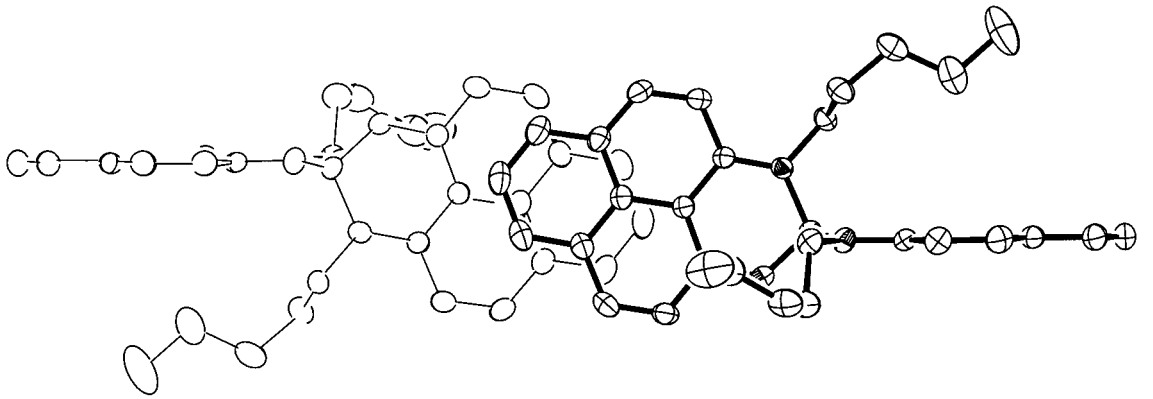

FIGURE 4. Overlap within a π-dimer of compound **4** (view normal to the two PLY units of the π-dimer).

dicular to each other (Fig. 6), the interactions between these molecules are weak and these columns cannot provide effective conducting pathways.

We have shown in Figures 2 and 4 that a unit cell contains four pairs of π-dimers. These dimer pairs also form columns along the b direction. The interaction between these dimer pairs in a column is illustrated in Figure 7.

The PLY units of neighboring π-dimers are perpendicular to each other, and thus the molecular interaction along the b direction is weak and this does not constitute an effective conducting pathway.

The molecular interaction along the c direction is illustrated in Figure 8, where the two molecules involved are H and J (Fig. 2). In this case, although the angle between the closest PLY units of H and J is comparable with those of radical **5,** these PLY units are in a side-by-side arrangement and the interaction between them is therefore weak.

Figure 9 shows the interaction between I and J. Again, the closest PLY units of these two molecules are side by side and their interaction must therefore be weak.

Figure 10 shows the interaction between I and K. The two closest PLYs are also side by side, with the larger distance d = 3.778 Å. This interaction must therefore be weak.

Molecules I and L are much farther away, with closest C . . . C contact larger than 7 Å. The interaction between them is therefore too weak to be considered.

From the above analysis, we can see that along the b direction (Figs. 5–7) some of the PLYs of neighboring molecules are directly above each other, but because they are perpendicular the interactions along this direction are weak. Both along the a and c directions (Figs. 8–10) the PLYs of neighboring molecules are all side by side and thus the interactions along these directions are even weaker. In summary, there are no continuous interactions between the molecules that are strong enough to provide effective conducting pathways.

BAND STRUCTURE OF PENTYL RADICAL (4)

Although there are certain objections to the application of tight-binding band theory to the neutral radical molecular conductors, we found that the calculated band dispersions in **1, 2, 3,** and **5** correlate qualitatively with their transport properties [5–7]. For example, the maximum dispersions are 0.036 eV (along a), 0.075 eV (along b), and 0.025 eV (along c) in **5,** with larger values in **1** and **3.** These radicals are good conductors, with comparable room temperature conductivities. The maximum dispersions in **2** are 0.03 eV (along a), 0.038 eV (along b), and 0.025 eV (along c). These lower values correlate with the lower conductivity found in **2.**

The extended Huckel theory (EHT) calculated band structure for **4** is shown in Figure 11. The 16 bands that are shown are derived from the nonbonding molecular orbitals of the 16 phenalenyl units in the unit cell.

The maximum dispersions are 0.01 eV (along a), 0.05 eV (along b), and 0.04 eV (along c). These values are significantly smaller than those of **1, 3,** and **5** but comparable with those of **2.** Thus, both the packing and the band calculation show this compound should be a poor conductor and similar in properties to radical **2.**

MAGNETIC SUSCEPTIBILITY OF PENTYL RADICAL (4)

We measured the magnetic susceptibility (χ) of **4** in the temperature range T = 4–320 K using a

TABLE III

Bond lengths of cation 3^+ [13], radical 4, and the referenced bond length of 4, together with the sign of partial bond order of SOMO [13, 14].

Bonds	Bond length (Å)			Bond length change (Å)	Environment of the PLY and SD[b]	Sign of partial bond order of SOMO
	Butyl cation (**3**$^+$)	Averaged[a] **3**$^+$	Pentyl radical (**4**)	**4**-averaged **3**$^+$		
C1—C2	1.413	1.411	1.412 (2)	0.001	PLY ring	+
C2—C3	1.358	1.36	1.362 (2)	0.002	involved in	−
C3—C3a	1.414	1.418	1.419 (2)	0.001	π-dimer (**4**);	+
C3a—C4	1.411	1.410	1.406 (2)	−0.006	SD = 0.003	−
C4—C5	1.37	1.373	1.374 (3)	0.001		0
C5—C6	1.388	1.388	1.386 (3)	−0.002		0
C6—C6a	1.392	1.389	1.396 (2)	0.007		−
C6a—C7	1.427	1.429	1.427 (2)	−0.002		+
C7—C8	1.346	1.346	1.349 (2)	0.003		−
C8—C9	1.437	1.439	1.441 (2)	0.002		+
C9—C9a	1.439	1.438	1.438 (2)	0		0
C9a—C1	1.401	1.4	1.399 (2)	−0.001		0
C9a—C9b	1.42	1.419	1.423 (2)	0.004		0
C9b—C3a	1.41	1.415	1.416 (2)	0.001		0
C9b—C6a	1.413	1.416	1.415 (2)	−0.001		0
C1—O1	1.326	1.33	1.327 (18)	−0.0026		−
B—O1	1.466	1.471	1.471 (2)	0		
C9—N9	1.336	1.335	1.3303 (19)	−0.0047		−
B—N9	1.534	1.543	1.575 (2)	0.032		
B—N19	1.552	1.543	1.512 (2)	−0.031	PLY ring not	
C19—N19	1.334	1.335	1.367 (2)	0.032	involved in	−
B—O11	1.476	1.471	1.450 (2)	−0.021	π-dimer (**4**);	
C11—O11	1.334	1.33	1.3538 (18)	0.0238	SD = 0.017	−
C19b—C16a	1.419	1.416	1.426 (2)	0.01		0
C19b—C13a	1.418	1.415	1.423 (2)	0.008		0
C19a—C19b	1.417	1.419	1.424 (2)	0.005		0
C19a—C11	1.399	1.4	1.407 (2)	0.007		0
C19—C19a	1.437	1.438	1.431 (2)	−0.007		0
C18—C19	1.44	1.439	1.408 (2)	−0.031		+
C17—C18	1.345	1.346	1.372 (2)	0.026		−
C16a—C17	1.431	1.429	1.411 (3)	−0.018		+
C16—C16a	1.387	1.389	1.413 (2)	0.024		−
C15—C16	1.389	1.388	1.388 (3)	0		0
C14—C15	1.376	1.373	1.373 (3)	0		0
C13a—C14	1.41	1.41	1.411 (2)	0.001		−
C13—C13a	1.42	1.418	1.411 (2)	−0.007		+
C12—C13	1.361	1.36	1.376 (2)	0.016		−
C11—C12	1.409	1.411	1.395 (2)	−0.016		+
SD[c]	0.0058		0.023			

[a] Each bond in a PLY unit (e.g., C1—C2) has a corresponding bond in the other PLY unit (C11—C12) related by the C_2 symmetry of the molecule. By averaging these two bonds, an averaged C1—C2 (or C11—C12) bond length is obtained.
[b] Standard deviation of the bond length changes of the radical referenced to the cation.
[c] Standard deviation of the bond lengths between the two halves of the molecule.

Faraday balance. Above 50 K the compound shows typical Curie–Weiss behavior with χ of the form: $\chi + \chi 0 + C/(T + \theta)$, leading to a temperature-independent diamagnetic contribution, $\chi 0 = -335.3 \times 10^{-6}$ emu/mol (equal to the calculated value), a Curie constant, $C = 0.356$ emu∗K/mol,

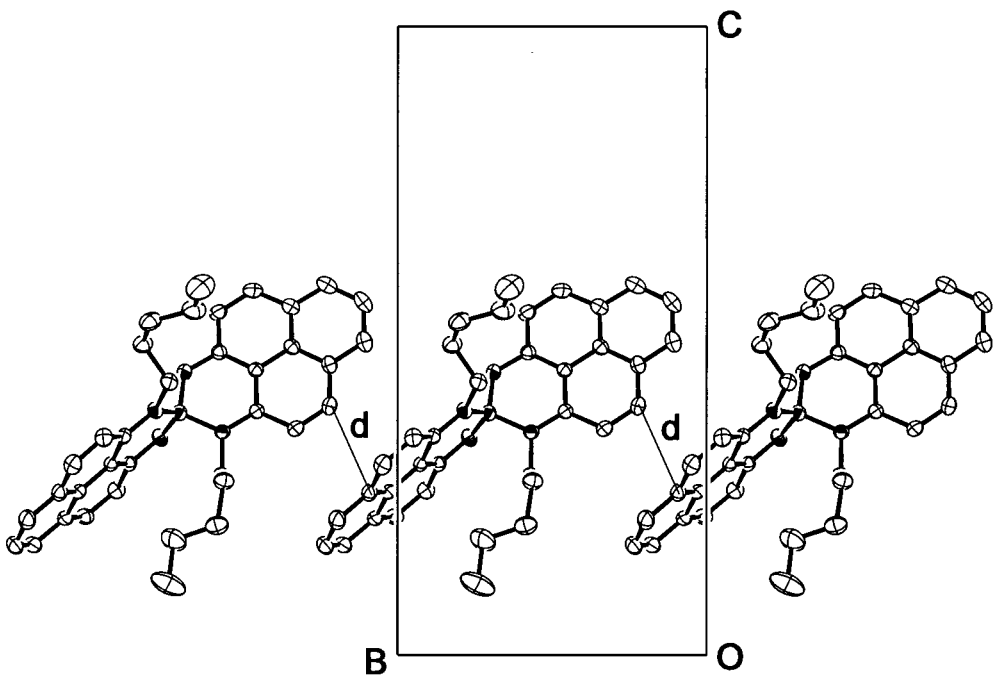

FIGURE 5. Each molecule in the unit cell, e.g., molecule **H,** forms a column along the b direction. The closest carbon–carbon contact distance: $d = 3.576$ Å.

and a Weiss constant, $\theta = 17$ K [Fig. 12(a)]. In Figure 12(b), we use the function $n = (\chi - \chi 0)(T + \theta)/0.375$ to obtain the number of Curie spins per molecule (n) for an $S = 1/2$ system as a function of temperature. The plot shows that in the solid state **4** behaves as a free radical with one spin per molecule, as expected from the structural analysis. At low temperatures weak intermolecular interaction at the energy scale of 17 K (1.5 meV) leads to antiferromagnetic ordering within the dimer at 30 K [Fig. 12(a)] and a decrease in the fraction of Curie spins per molecule [Fig. 12(b)].

ELECTRICAL CONDUCTIVITY OF PENTYL RADICAL (4)

Single crystal conductivity measurements were performed using a four-probe configuration. Figure 13 represents the temperature dependence of the conductivity. The conductivity shows semiconducting temperature dependence with activation energy 0.45 eV, significantly higher than in **5** (0.13 eV [5]). The value of the room temperature conductivity of **4,** $\sigma_{RT} = 4 \times 10^{-7}$ S/cm, is five orders of magnitude lower than in compound **5** [5].

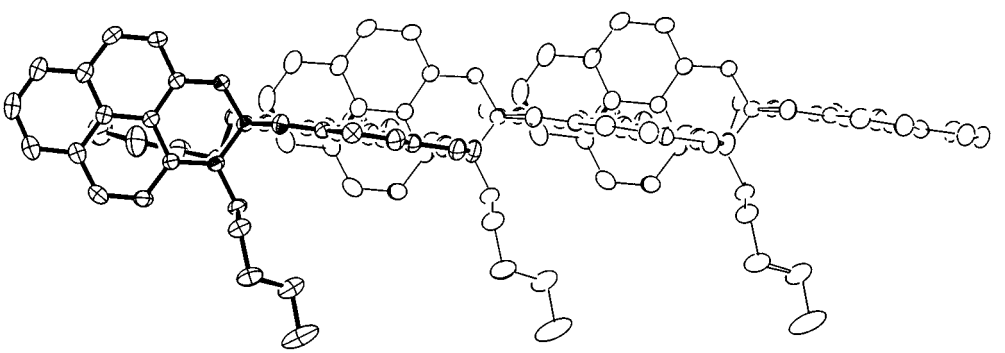

FIGURE 6. PLY units of neighboring molecules in the column (Fig. 5) are perpendicular to each other. Viewing normal to the plane of the left half of the molecules.

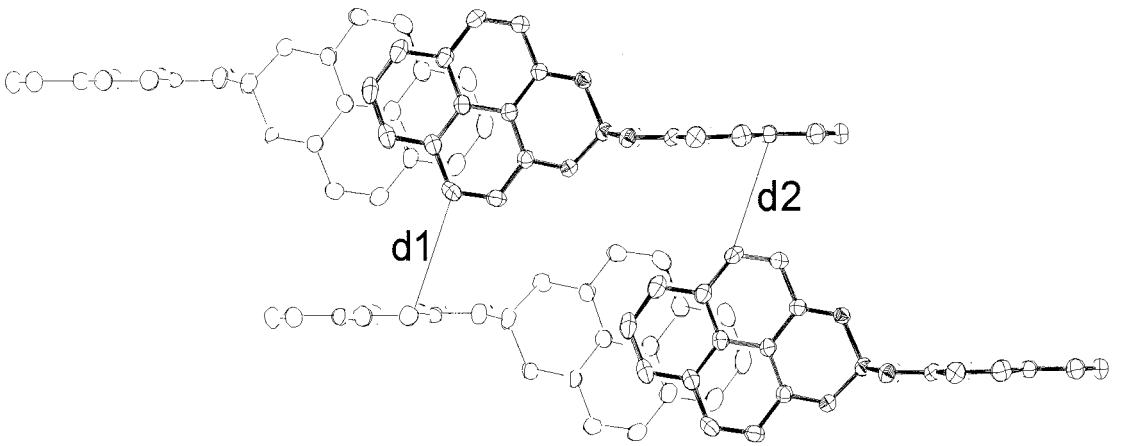

FIGURE 7. Two neighboring pairs of π-dimers in a column formed by H and I (Fig. 2) along the b direction, viewed normal to the planes of the PLY units that have π–π interactions. The closest carbon–carbon contacts are $d1$ = 3.74 Å and $d2$ = 3.47 Å.

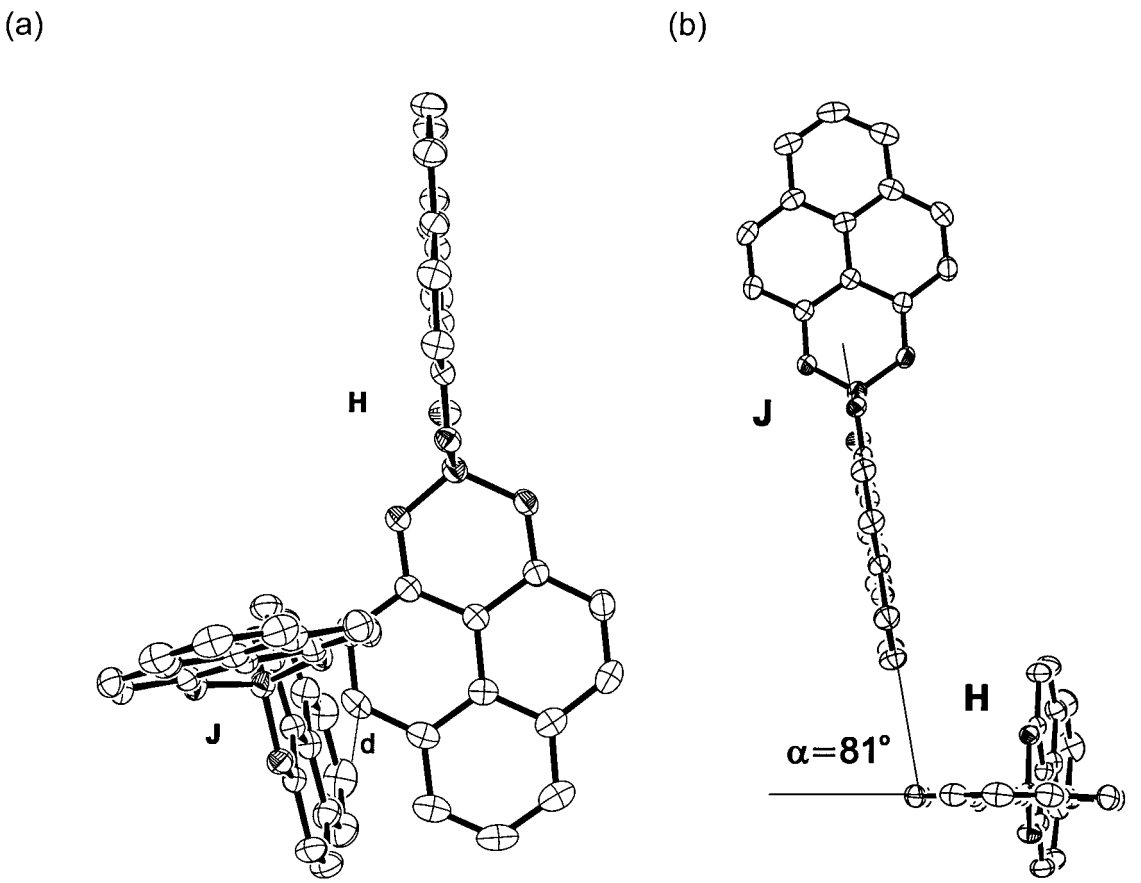

FIGURE 8. Interactions between molecules J and H (Fig. 2). (a) View normal to the plane of the bottom half of molecule H. Note that the bottom half of molecule J has closest contact with molecule H (d = 3.651 Å) and they are to the side of each other. (b) View normal to the top half of molecule J.

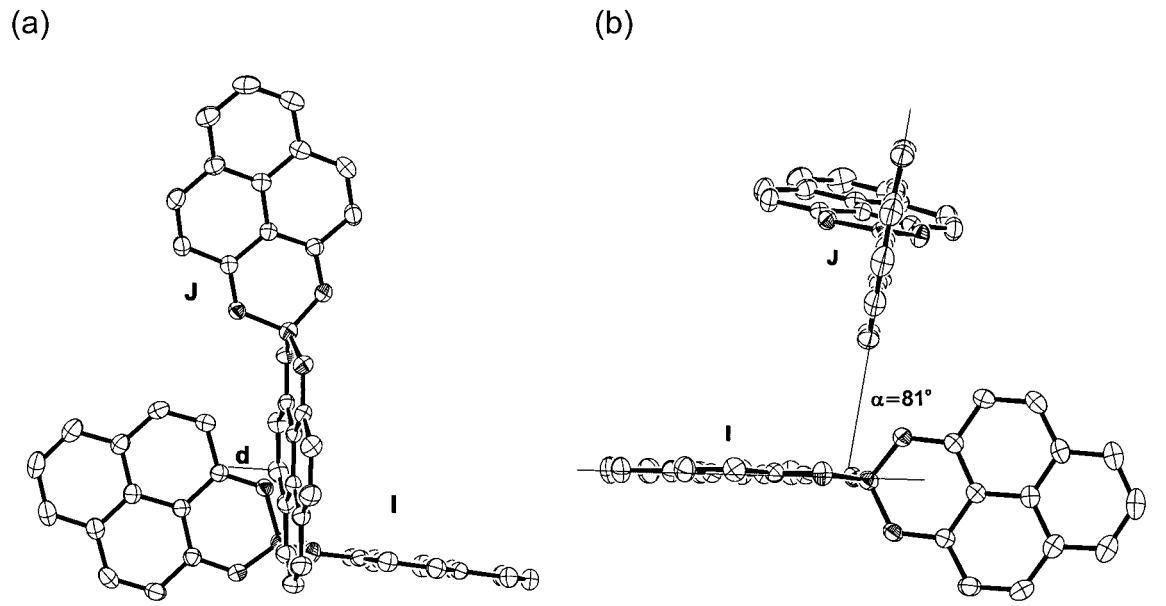

FIGURE 9. Interaction between I and J. (a) View perpendicular to the left PLY unit of I, which has closest C . . . C contact with the bottom PLY of J with $d = 3.881$ Å and these two PLY units are side by side. (b) View perpendicular to the right half of molecule I. α is the angle between the two closest PLY units of I and J.

OPTICAL MEASUREMENTS OF PENTYL RADICAL (4)

Figure 14(a) represents the room-temperature transmission spectrum of a single crystal of pentyl radical **4** in the spectral range 650–10,000 cm^{-1}. It shows a strong increase of absorption between 0.41 and 0.57 eV, similar to the fundamental absorption edge in conventional semiconductors. The absorptions in the mid-IR (infrared) between 650 and 3100 cm^{-1} are due to molecular vibrations of radical **4.**

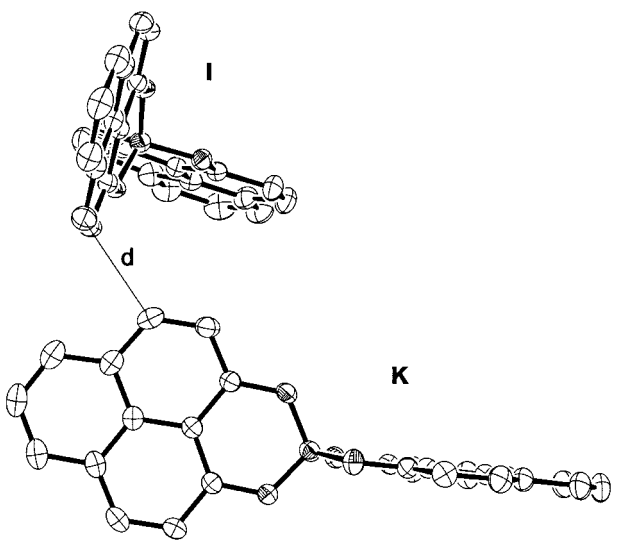

FIGURE 10. Interaction between I and K. View perpendicular to the left half of K. The PLY of I that is toward us has the closest C . . . C contact with the left PLY of K, with $d = 3.778$ Å. These two PLY units are side by side.

The measured optical bandgap (E_g) usually correlates with the activation energy (Δ) calculated from the temperature dependence of the conductivity, so that $E_g = 2\Delta$ if electrons and holes contribute to the conductivity. Surprisingly, the optical data of **4** is similar to that of **5** [5] with the absorption edge starting at almost the same energy [$E_g = 0.4$ eV; see Fig. 14(a)], while the activation energies of the conductivity (Δ) of **4** and **5** [5] differ by more than a factor of 3. To better understand the nature of the observed near-IR (NIR) absorption of **4,** we performed a solution IR measurement of **4** in acetonitrile [Fig. 14(b)]. Comparison of Figures 14(a) and 14(b) shows that the absorption band of the single crystal correlates with the first absorption peak in the solution spectrum. The solution phase absorption [Fig. 14(b)] arises from excitation from the SOMO to the lowest unoccupied molecular orbital (LUMO). This pair of orbitals (SOMO and LUMO) results from the spiro-interaction between the symmetrical and antisymmetrical combinations of the 1,9-disubstituted-phenalenyl nonbonded molecular

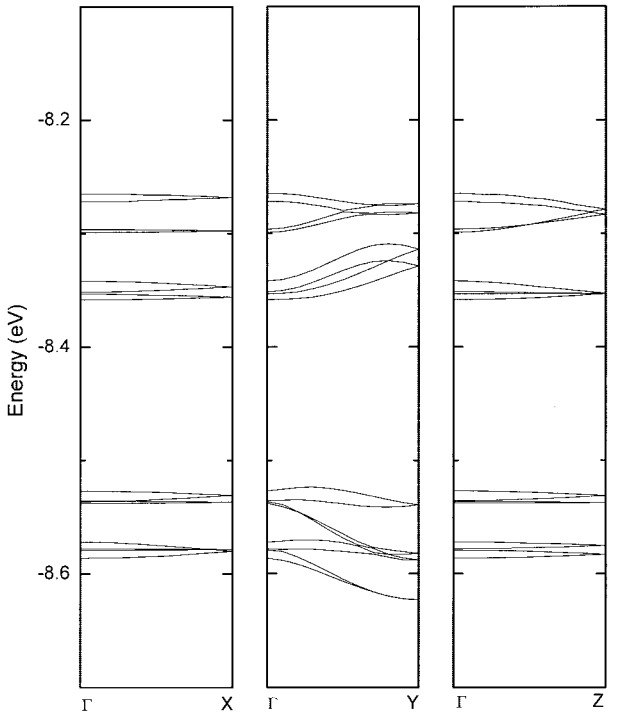

FIGURE 11. Calculated band structure for crystalline pentyl radical (**4**).

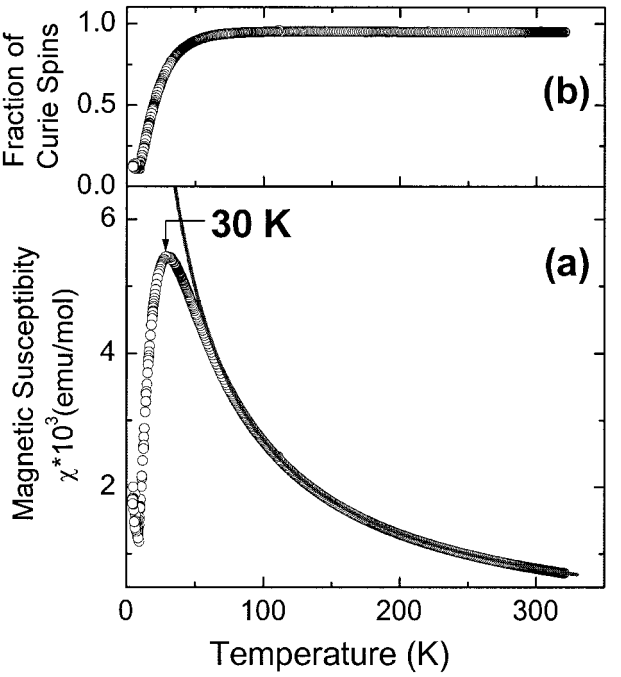

FIGURE 12. (a) Magnetic susceptibility of radical **4** as a function of temperature (open circles). The solid line is a Curie–Weiss fit to the data between 70 and 320 K. (b) Fraction of Curie spins per molecule (see text) as a function of temperature.

orbitals (NBMOs) [14]. The similarity of the absorption features in the solid and solution states suggests that the absorption spectrum of the crystalline state is due in large part to molecular transitions. Thus, the association of the molecules in the crystal lattice in the solid state does not strongly modify the electronic structure of the individual molecules, in agreement with the weak intermolecular interactions suggested by the band structure calculations.

In a previous article [5], we proposed that crystalline **5** corresponds to degenerate Mott–Hubbard insulator with a localized ground state. This model can be extended to the whole class of spiro-biphenalenyl boron neutral radicals [5–7], including the pentyl compound **5.** This model naturally accommodates the Curie-type magnetic susceptibility behavior with one independent spin per molecule observed in these compounds (excluding the strongly dimerized state in **1, 3,** and **4**).

Typically, the conductivity in molecular conductors depends strongly on the on-site Coulomb correlation energy U. The activation energy of the conductivity, $\Delta = 0.45$ eV, in **4** may be associated with U ($U = \Delta$) [5]. However, U is primarily a molecular property, and thus there is no reason to expect different values of U for radicals **4** and **5,** whereas we find $\Delta = 0.45$ and 0.13 eV, respectively. Thus, it may be that the bare value of U provides an upper bound for Δ but that this is subject to modification by subtle features of the band structure. The temperature dependence of the mobility of charge carriers can also affect the observed value of Δ [5].

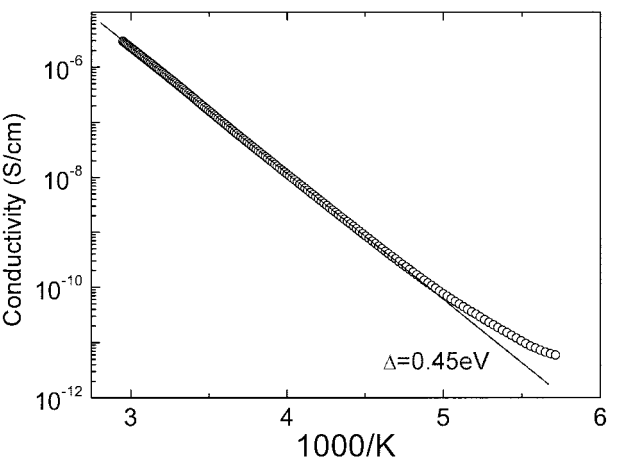

FIGURE 13. Single-crystal conductivity of **4** as a function of temperature.

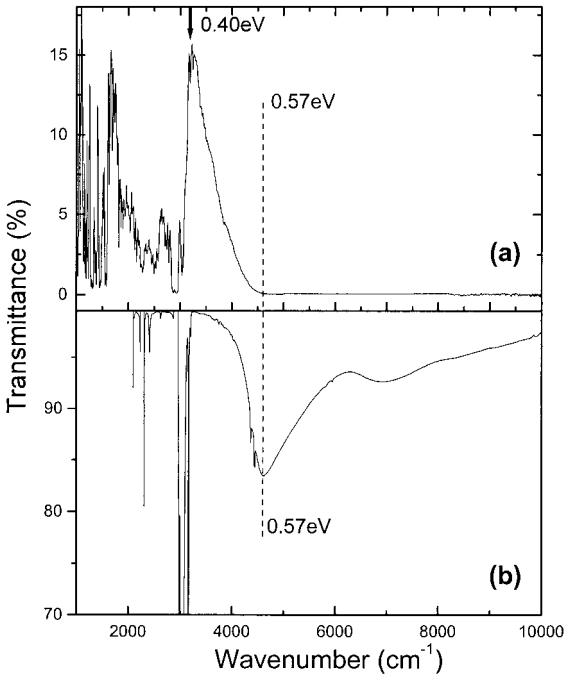

FIGURE 14. Near- and mid-IR transmission spectra of (a) single crystal of pentyl radical (**4**) and (b) solution of (**4**) in acetonitrile.

At present, the mechanism of conductivity within the entire family of spiro-biphenalenyl boron neutral radicals, including the relationship between the conductivity gap Δ, the optical gap E_g, and the on-site Coulomb correlation energy U, is not well understood.

Conclusion

The low disproportionation energies—which largely determine the on-site Coulomb correlation energy in the solid state—suggest that these spiro-biphenalenyl boron complexes possess great potential for the development of organic conductors and superconductors. The conductivity of the solid formed by the radical is largely determined by the molecular packing. By changing the length of the alkyl groups, we obtained a series of neutral radicals that have a unique set of properties. Some of them are poor conductors without effective conducting pathways; others are among the most highly conducting neutral organic solids. The radicals form conducting pathways in a more complicated manner than in the classic organic conductors (TTF derivatives and C_{60} charge-transfer salts) and the intermolecular interactions are much weaker. Nevertheless, we have been able to compare the interactions of the molecules in the crystal lattice and find evidence for the directions that can conduct effectively. In these solids the relationship between structure, magnetism, and conductivity are much more subtle than in the charge-transfer salts.

New compounds can be readily synthesized by changing the alkyl groups, and there are many opportunities for the preparation of novel neutral radicals. The goal is to crystallize a neutral radical with a reduced disproportionation energy and a better packing structure (more effective conducting pathway), and thereby produce intrinsic molecular metals and superconductors.

ACKNOWLEDGMENTS

This work was supported by the Office of Basic Energy Sciences, Department of Energy, under Grant DE-FG03-01ER45879 and by Los Alamos National Laboratories Grant STB-UC:10019-001.

References

1. Williams, J. M.; Ferraro, J. R.; Thorn, R. J.; Carlson, K. D.; Geiser, U.; Wang, H. H.; Kini, A. M.; Whangbo, M.-H. Organic Superconductors (Including Fullerenes); Prentice-Hall: Englewood Cliffs, NJ, 1992.
2. Tanaka, H.; Okano, Y.; Kobayashi, H.; Suzuki, W.; Kobayashi, A. Science 2001, 291, 285–287.
3. Haddon, R. C. Nature 1975, 256, 394–396.
4. Oakley, R. T. Can J Chem 1993, 71, 1775–1784.
5. Chi, X.; Itkis, M. E.; Patrick, B. O.; Barclay, T. M.; Reed, R. W.; Oakley, R. T.; Cordes, A. W.; Haddon, R. C. J Am Chem Soc 1999, 121, 10395–10402.
6. Chi, X.; Itkis, M. E.; Kirschbaum, K.; Pinkerton, A. A.; Oakley, R. T.; Cordes, A. W.; Haddon, R. C. J Am Chem Soc 2001, 123, 4041–4048.
7. Chi, X.; Itkis, M. E.; Reed, R. W.; Oakley, R. T.; Cordes, A. W.; Haddon, R. C. J Phys Chem B 2002, 106, 8278–8287.
8. Haddon, R. C.; Wudl, F.; Kaplan, M. L.; Marshall, J. H.; Cais, R. E.; Bramwell, F. B. J Am Chem Soc 1978, 100, 7629–7633.
9. Haddon, R. C.; Rayford, R.; Hirani, A. M. J Org Chem 1981, 46, 4587.
10. Cordes, A. W.; Haddon, R. C.; Oakley, R. T.; Schneemeyer, L. F.; Waszczak, J. V.; Young, K. M.; Zimmerman, N. M. J Am Chem Soc 1991, 113, 582.
11. Haddon, R. C.; Siegrist, T.; Fleming, R. M.; Bridenbaugh, P. M.; Laudise, R. A. J Mater Chem 1995, 5, 1719–1724.
12. Robbins, J. L.; Edelstein, N.; Spencer, B.; Smart, J. C. J Am Chem Soc 1982, 104, 1882–1893.
13. Chi, X.; Tham, F. S.; Cordes, A. W.; Itkis, M. E.; Haddon, R. C. Synth Metals 2003, 133/134, 367–372.
14. Haddon, R. C.; Chichester, S. V.; Marshall, J. H. Tetrahedron 1986, 42, 6293–6300.